

Investigations beyond the standard model

G Amar

National Institute for Theoretical Physics, School of Physics, University of the Witwatersrand,
South Africa

E-mail: gilad.amar@cern.ch

Abstract. The LHeC, a possible addition to the LHC, allows for electron beams within the LHC. In this report new possibilities for investigating physics beyond the Standard Model with the LHeC are explored. An investigation of anomalous Higgs couplings in electron and positron collisions is presented, with promising results for detection of beyond Standard Model physics using the LHeC.

1. Feasibility study for beyond Standard Model research

The LHeC is a proposed project investigating the possibility of extending the collision types and energies at the LHC. The idea for achieving a wider range of collision possibilities is realized by colliding an electron beam from a new accelerator with the already existent proton beam of the LHC. Preliminary studies indicate that a luminosity of $10^{33} \text{ cm}^{-2}\text{s}^{-1}$ would be possible, with a centre of mass energy beyond 1 TeV [1].

There are a number of proposed designs for the LHeC layout. The first is a new electron ring on top of the current proton ring in the LHC tunnel, this yields the largest luminosities of the considered designs. Such an electron accelerator based inside the LHC tunnel can conceivably produce an electron beam of 50 GeV and a luminosity of $5 \times 10^{33} \text{ cm}^{-2}\text{s}^{-1}$ which corresponds to an integrated luminosity of order 100fb^{-1} . Alternatively, a linear accelerator can be used instead. The advantages of such a design include the construction of the LHeC to be largely separate from the existing LHC site, reducing complexity and cost, and larger electron beam energies are a possibility [2]. Energies up to 150 GeV are in consideration, with the design largely limited by cost. In contrast with the electron ring design, the linear accelerator may provide an electron beam of 150 GeV, a luminosity of $5 \times 10^{32} \text{ cm}^{-2}\text{s}^{-1}$ and an integrated luminosity of order 10fb^{-1} . Of course, in either case, there is the added possibility of using a lead ion beam instead of protons further increasing the range of possible collision types and energies. In the example of the electron-ring LHeC, 2.7 TeV per nucleon is likely with a luminosity of $10^{31} \text{ cm}^{-2}\text{s}^{-1}$.

Physics programs stand to gain a lot from the LHeC. For example, the largely unexplored Standard Model (SM) processes which have prohibitively small cross-sections with the current LHC set-up can now be studied. These include the production of a light Higgs and a single top-quark. Undiscovered particles and new physics on distance scales below 10^{19}m are more sensitive to being probed. Promising channels include lepton-quark bound states, super-symmetric electrons and excited leptons. The determination of nucleon structure with greater precision is now a possibility, fixing the poor knowledge of gluon density and d/u quark ratio. In addition, more precise measurements of the SM electroweak and strong parameters can be made. Using

heavy-ion beams instead of protons opens the door to further measurement of the deep inelastic structure of nuclei which would be a welcome change from the previous lepton-nucleon scattering experiments which relied on xed target nucleons. Measurements of this kind would be four orders of magnitude larger beyond the accessible kinematic range of prior experiments.

1.1. Investigating Beyond the SM

Symmetry breaking is transmitted from the scalar sector to the gauge sector by having gauge boson-scalar couplings from the assignment of non-trivial gauge quantum numbers to the scalar fields in the theory. The precise couplings of the SM Higgs to the heavy electroweak gauge bosons W^\pm and Z come out as

$$L_{int} = -gM_W \left(W_\mu W^\mu + \frac{1}{2\cos\theta_W} Z_\mu Z^\mu \right) H. \quad (1)$$

The constants g , M_W and θ_W are all accurately measured, this vertex being fully determined in the SM. In confirming that the SM mechanism for breaking electroweak symmetry is the correct one, independent measurement of these vertices is required. In addition to these vertices requiring copious amounts of Higgs production for convincing statistical results, these vertices are also sensitive to Beyond Standard Model (BSM) physics. The $H(k)W^+(p)W^-(q)$ vertex can be parametrised in the following form [3]

$$i\Gamma^{\mu\nu}(p, q)\epsilon_m u(p)\epsilon_\nu^*(q). \quad (2)$$

Deviations from the SM form of $\Gamma_{SM}(p, q) = gM_W g$ would indicate the presence of BSM physics. These BSM deviations can be specified using the following formula

$$\Gamma_{\mu\nu}^{BSM}(p, q) = \frac{g}{M_W} [\lambda(p \cdot q g_{\mu\nu} - p_\nu q_\mu) + \lambda' \epsilon_{\mu\nu\rho\sigma} p^\rho q^\sigma] \quad (3)$$

where λ and λ' are the effective strengths for the anomalous CP-conserving and CP-violating operators respectively. Whilst the CP properties are difficult to measure directly, they can be known if the couplings λ and λ' can be determined with good precision and accuracy.

1.2. Computational Research

The computational research in this paper will analyse the $e^+ + e^- \rightarrow h + \nu + \bar{\nu}$ process and see if there are any BSM physics involved. MadGraph 1.5.9, a program used to do Monte Carlo simulations allowing the user to calculate cross sections and to obtain unweighted events, was installed [4]. FeynRules is a Mathematica package that allows the calculation of Feynman rules in momentum space for any QFT physics model [5]. The minimal information to describe the new model including BSM higgs couplings is contained in the model-file. This information is then used to calculate the Feynman rules associated with the Lagrangian. The Feynman rules generated are then implemented into MadGraph. The number of events to be simulated were set to 100000. The programming framework ROOT was used to generate histograms. ROOT is a system environment and set of libraries developed by CERN designed specifically for particle physics data analysis [6]. Simulated event data is stored in .lhe files. The Les Houches Events (LHE) file format is an agreement between Monte Carlo event generators and theorists to define Matrix Element level event listings in a common language [7]. Adding the Pythia extension to MadGraph allows MadGraph to store the events, usually in a .lhe extension in .root files [8]. The different format being more easily used within the ROOT framework. All events utilise what is known as a Monte Carlo Numbering Scheme. This convention facilitates communication between event generators, detectors and analysis packages.

1.3. Results and Analysis

There are two channels in which the process $e^+ + e^- \rightarrow h + \nu_e + \bar{\nu}_e$ can occur. An S-channel is the joining of colliding particles into an intermediate particle that eventually splits into other particles. A T-channel is where two colliding particles interact via the emission of an intermediate particle from one of them. The S-channel features the production of the neutrinos through the decay of a Z boson.

$$e^+ + e^- \rightarrow z \rightarrow h + \nu_e + \bar{\nu}_e. \quad (4)$$

This means that the simulated events for the production of the Higgs and two neutrinos must come from the production of a Z boson that decays. In contrast the T-channel features the production of the Higgs and neutrino pair through vector boson fusion.

$$e^+ + e^- \rightarrow h + \nu_e + \bar{\nu}_e \setminus Z. \quad (5)$$

The $\setminus Z$ denotes that processes contributing to the final state resulting from the decay of the Z boson are excluded. In understanding what contributions to the complete process are made from the two channels it is possible to learn how to distinguish between the sources of the data that are accrued by the detector.

Having run simulations of the two channels separately histograms were plotted for a beam energy of 125 GeV . At the centre of mass (COM) energy of 250 GeV, five different simulations were done. All differed on the strength of the factors λ and λ' using values of ± 1 . For all the histograms that follow, the SM plot is in black for convenience of easy distinction from the coloured, or BSM, physics. λ equal to one and negative one are red and green respectively. λ' equal to one and negative one are purple and blue respectively.

Two histogram plots were selected for their useful insights and strikingly apparent differences between the physics models. Those selected are of the Higgs angle phi (azimuthal angle distribution w.r.t. the reaction plane defined by the incident particles) and a two-dimensional histogram showing the correspondence between theta (angle between collision product and incident beam) and momentum of the Higgs [9]. Histograms featuring properties of the emitted neutrinos were omitted as they, whilst showing appreciable differences, are near impossible to investigate with the detectors of the LHC. The S-channel features a Gaussian distribution centred

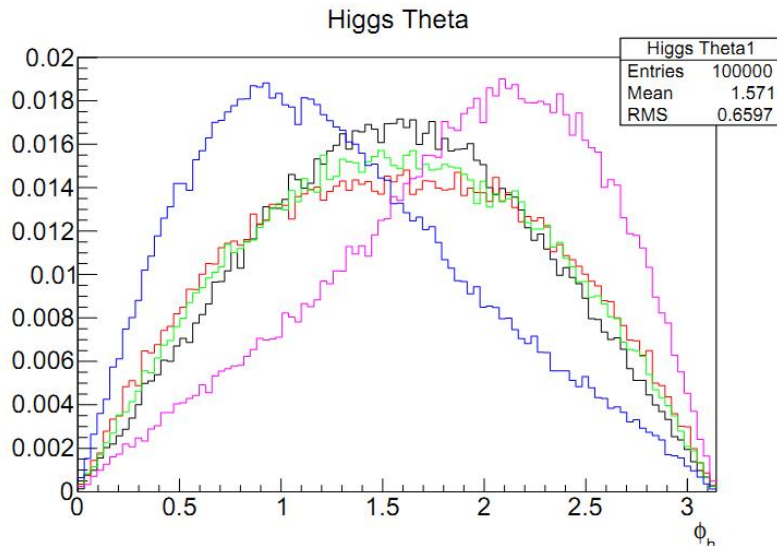


Figure 1. Higgs theta distribution from the S-channel at COM energy of 250 GeV.

around 61 GeV . This makes for easy separation of the two channels by merely excluding all

measurements of the Higgs momentum in near the peak. A quick glance at the Higgs theta distribution shows that the $\lambda = \pm 1$ processes differ slightly to the SM prediction, however the $\lambda' = \pm 1$ processes introduce a strong asymmetry about the line $\theta = \frac{\pi}{2}$ which can be used to determine if the true value of λ is non-zero. The two-dimensional histogram highlights the spike in momentum-theta phase space for the S-channel.

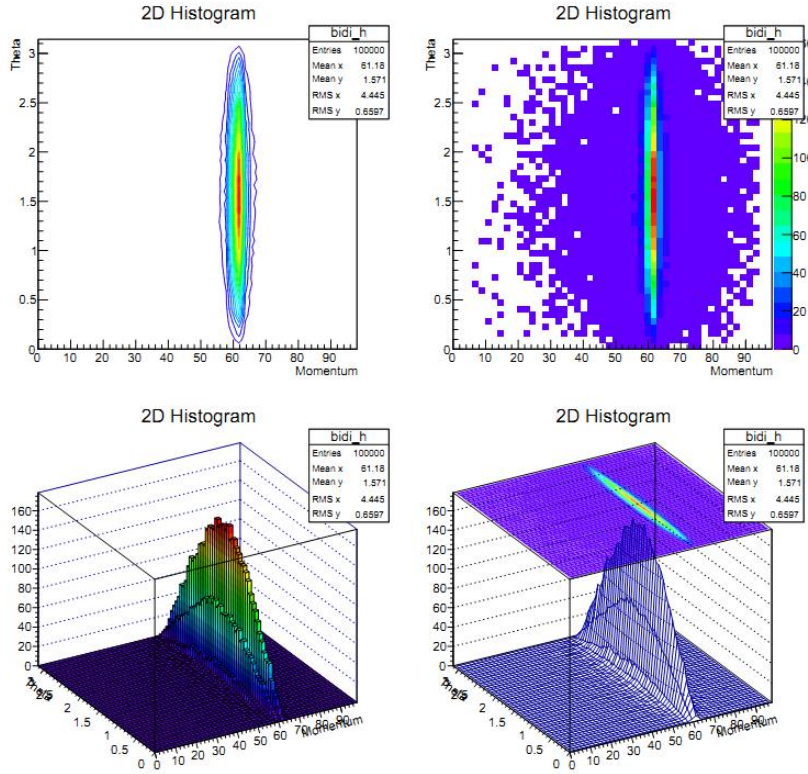


Figure 2. Two-dimensional histogram showing the correlation of the S-channel Higgs momentum and theta at COM energy 250 GeV.

In contrast with the S-channel, it can be seen that the T-channel Higgs momentum has a wide range of accessible values. So in excluding the peak of the S-channel it is quite possible to explore the T-channel and any variations from the SM. Compared to the S-channel, we see all the BSM parameters do affect the T-channel Higgs theta distribution, but unfortunately no asymmetry about $\frac{\pi}{2}$ which can be exploited as in the case of the S-channel. It is apparent in the T-channel that there is a much more widely distributed momentum and theta correlation than that of the S-channel. As you can see, what makes for a very effective separation of the signal from the background is that the S-channel features a very strong peak of the Higgs momentum at a certain energy. In cutting out the momentum window it is not so simple as excluding a particular range of detected events without considering the specifics of the detector. The momentum of the Higgs particle cannot be measured directly as it decays very rapidly. Primarily decaying to a $b\bar{b}$ quark pair, each producing a jet of particles, it is the measured momentum of these jets that tells us about the momentum of the initial Higgs boson. The resolution of the initial energy of the b quark has been found to be $\frac{60\%}{\sqrt{E}}$, the resolution of the Higgs momentum, the sum of the two b-jets is then given by $\sqrt{2}\frac{60\%}{\sqrt{E}}$. In excluding a two sigma E window on either side of the peak we ensure that 95% of the events within the range are cut out, however there will be a

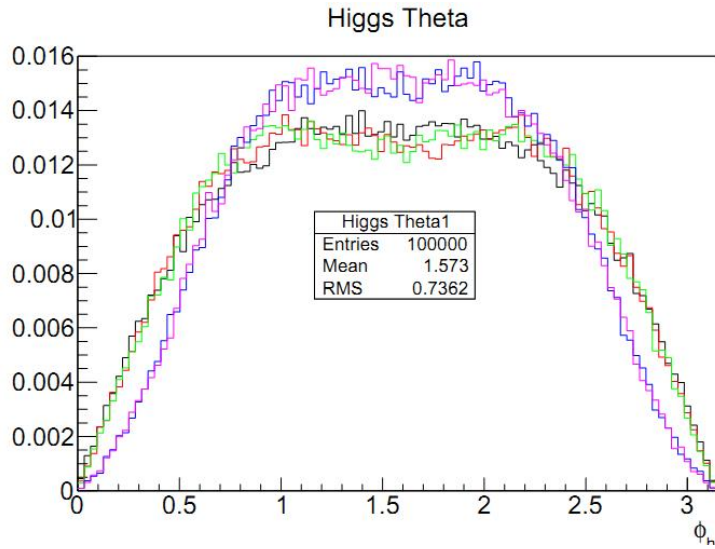


Figure 3. Higgs theta distribution from the T-channel at COM energy of 250 GeV.

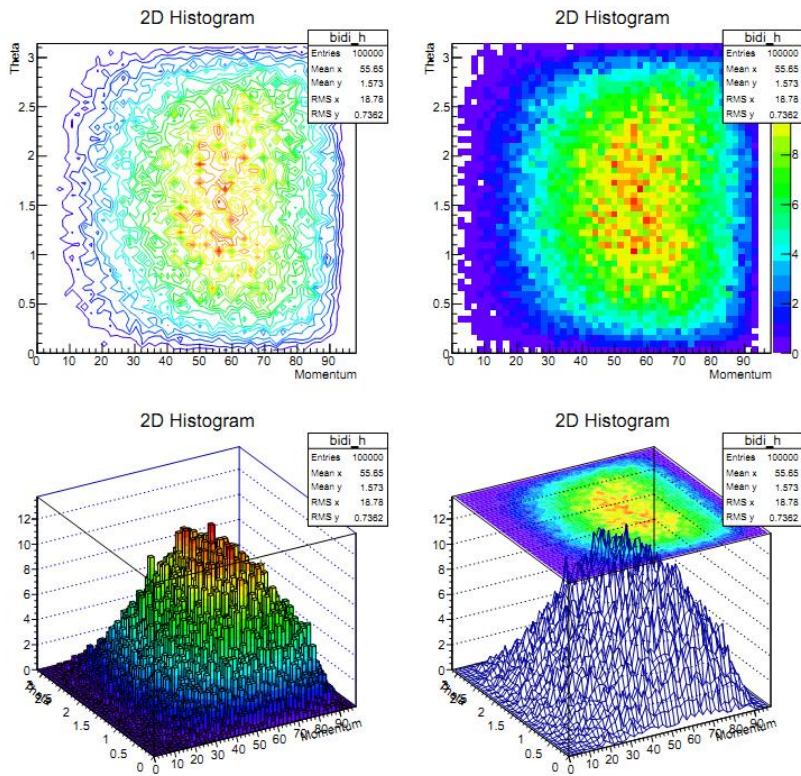


Figure 4. Two dimensional histogram showing the correlation of the T-channel Higgs momentum and theta at COM energy 250 GeV.

5% migration of some events that were within the window, being detected as having been from without.

The cross-sections are given from the outcome of the MadGraph run. Such output will have

to be modified by the cuts we imposed and other considerations. In all the simulations the output state was declared to involve an electron and anti-electron neutrino pair. However the lepton universality allows for end-states involving tau and muon neutrino pairs also, as such the MadGraph given cross-section needs to be multiplied by three. The cuts on the allowed momentum too will affect the cross-section. The fraction of events that survive the cut, times the cross-section signifies the cross-section for the process. Finally, the Higgs to $b\bar{b}$ branching ratio of 57.7% must also be considered. This simply means that the cross-section must be multiplied by 0.577.

1.4. Prospects for the future

Many avenues of further research still remain. Using results derived from Wilks and Wald, confidence intervals on the model parameters can be obtained, accounting for systematic uncertainties in test procedures. In this way the results of the experiment, especially the two-dimensional distributions, can be used to determine the values of λ and λ' even possibly finding them to be complex valued which was not explored in this paper. As with any simulation, higher order corrections may be explored, increasing accuracy at the cost of CPU time. Higher order corrections would be the inclusion of more Feynman diagrams and the multiple decay paths of the Higgs. The study was almost entirely focused on the parton-level, a more comprehensive and involved study would include the Higgs decay and hadronization of the resultant jets. Finally, it should not be said that all criterion useful for evaluating the BSM parameters were discovered. For instance, the asymmetry in Higgs theta distribution as a result of λ' values may be exploited to further increase the accuracy obtained from the two dimensional distributions.

2. Conclusion

In conclusion, it is seen that the existence of BSM physics parameters can make a significant and detectable difference to Higgs production. A useful ratio was discovered to test differences from the SM and with further statistical based work can be expanded to determine BSM parameters and their respective confidence intervals. The construction of the LHeC would go a long way toward studying BSM physics in a significantly less convoluted way than the LHC alone could.

Acknowledgments

Acknowledgments The research in this paper was conducted as part of a internship for the National Institute of Theoretical Physics (NITheP) under the supervision of Dr. Alan Cornell. I sincerely appreciate Dr. Cornell and my co-supervisor, Prof. Bruce Mellado for their valuable insight and guidance. I am indebted to Kirtimaan Mohan for introducing me to Madgraph and providing me with his FeynRules. Finally I wish to thank NITheP, in particular to Renè Kotzè for having organized the internship.

References

- [1] O. Bruening and M. Klein, Mod. Phys. Lett. A **28**, no. 16, 1330011 (2013) [arXiv:1305.2090 [physics.acc-ph]].
- [2] P. Newman, Nucl. Phys. Proc. Suppl. **191**, 307 (2009) [arXiv:0902.2292 [hep-ex]].
- [3] A. Djouadi, R. M. Godbole, B. Mellado and K. Mohan, Physics Letters B **723**, , pp. 307 (2013) [arXiv:1301.4965 [hep-ph]].
- [4] <http://madgraph.phys.ucl.ac.be/>
- [5] N. D. Christensen and C. Duhr, Comput. Phys. Commun. **180**, 1614 (2009) [arXiv:0806.4194 [hep-ph]].
- [6] <http://root.cern.ch/drupal/>
- [7] J. Alwall, A. Ballestrero, P. Bartalini, S. Belov, E. Boos, A. Buckley, J. M. Butterworth and L. Dudko *et al.*, Comput. Phys. Commun. **176**, 300 (2007) [hep-ph/0609017].
- [8] <https://pythia6.hepforge.org/>
- [9] A. R. Baden, Int. J. Mod. Phys. A **13**, 1817 (1998).